Available online at www.sciencedirect.com
SCIENCE DIRECT
Applied Surface Science 210 (2003) 32–36
applied surface science
www.elsevier.com/locate/apsusc

Resolution of Kelvin probe force microscopy in ultrahigh vacuum: comparison of experiment and simulation

S. Sadewasser[a,*], Th. Glatzel[a], R. Shikler[b], Y. Rosenwaks[b], M.Ch. Lux-Steiner[a]

[a]*Hahn-Meitner Institut Berlin, Glienicker Str. 100, 14109 Berlin, Germany*
[b]*Department of Physical Electronics, Tel-Aviv University, Ramat-Aviv 69978, Israel*

Abstract

An ultrahigh vacuum Kelvin probe force microscope (UHV-KPFM) is used to image the work function change of semiconductor surfaces. We measured the potential drop across the pn-junction on a GaP (1 1 0) surface and the potential variation at steps on the GaAs (1 1 0) surface and determined the resolution for different tip–sample distances. A simple parallel plate capacitor model is used to simulate the effect of varying tip–sample distance on the detection of the electrostatic forces between tip and sample. The model is applied to a potential step and a potential line. The results for different tip–sample distances are compared to those of the experiment; despite small deviations this simple model describes the experimental situation reasonably well. From the simulations it is concluded that for operation of KPFM in air a serious limitation in resolution has to be accepted.

PACS: 07.79.L; 61.16.C

Keywords: Electrostatic force; KPFM; Work function; AFM

1. Introduction

As the size of structures in modern electronics continuously decreases, the need for nanoscale characterisation techniques grows. Scanning probe microscopy (SPM) allows to study samples with nanometer, even down to atomic resolution [1]. The Kelvin probe force microscope (KPFM) measures the contact potential difference (CPD), which is the difference in work function between tip and sample and reaches high lateral and energy resolution [2,3]. Application in ultrahigh vacuum (UHV) improves the lateral resolution, so that even atomic resolution for the CPD has been reported [4–6]. However, the resolution limits of KPFM images are discussed diversely. For example, for pn-semiconductor structures the observed CPD contrast is usually considerably smaller than expected [7,8]. For studies in air, surface contamination can result in a reduced CPD contrast. The geometry of the probe (consisting of tip and cantilever) could average the signal, due to the long range nature of the electrostatic force; this effect persists for clean samples studied under UHV conditions. A variety of studies to model these effects of tip and cantilever on the electrostatic forces have been conducted, some using analytical estimates for simplified tip geometries, others simulating the cantilever–tip–sample system with various approaches [9–12]. The studies obtain

* Corresponding author. Tel.: +49-30-8062-2164; fax: +49-30-8062-3199.
E-mail address: sadewasser@hmi.de (S. Sadewasser).

0169-4332/03/$ – see front matter © 2003 Elsevier Science B.V. All rights reserved.
doi:10.1016/S0169-4332(02)01475-7

varying results for the resolution of KPFM, and the importance of the cantilever effect.

In this paper we will present results of ultrahigh vacuum Kelvin probe force microscope (UHV-KPFM) measurements on III–V semiconductor surfaces, studying the work function variation across a GaP pn-junction and at steps on the surface of GaAs. We compare these to results of a simple parallel plate capacitor model to simulate the resolution at a potential step and a potential line.

2. Experimental details

2.1. UHV-KPFM

For KPFM, a regular noncontact atomic force microscope (NC-AFM) is modified to allow additionally the measurement of electrostatic forces [2]. For this purpose, a dc bias V_{dc} and an ac voltage $V_{ac}\sin(\omega t)$ are applied between tip and sample. The ac voltage induces oscillatory electrostatic forces: $F_{es} = -(1/2)\partial C/\partial z\, V^2$, to which the spectral component at the frequency ω of the ac voltage contributes as [13]

$$F_\omega = \frac{\partial C}{\partial z}\left(V_{dc} - \frac{\Delta\Phi}{e}\right)V_{ac}\sin(\omega t) \quad (1)$$

where $\partial C/\partial z$ is the capacitance gradient between probe and sample and $\Delta\Phi/e = (\Phi_{sample} - \Phi_{tip})/e$ is the CPD. The oscillation at ω is detected using a lock-in amplifier and a controller is used to reduce the amplitude to 0 by adjusting V_{dc} to match the CPD.

The present KPFM is a modified UHV-AFM (Omicron) operated at $p \le 10^{-10}$ mbar [14]. The topography is measured using the regular frequency modulation technique at the first cantilever resonance frequency (~75 kHz) and the ac voltage is tuned to the second resonance frequency, thereby allowing a highly sensitive, simultaneous and independent detection of the electrostatic forces: applying low ac voltages (100 mV), still high energy (~5 meV) and lateral resolution (~20 nm) are maintained [13].

The pn-junction was prepared by growing a p-type GaP layer (p ~1.5×10^{18} cm^{-3}) using liquid phase epitaxy onto a n-type GaP wafer (n ~5×10^{17} cm^{-3}). For the experiments on the steps, we used n^+-type GaAs(0 0 1) wafers. All samples were cleaved in UHV to expose the (1 1 0) surface.

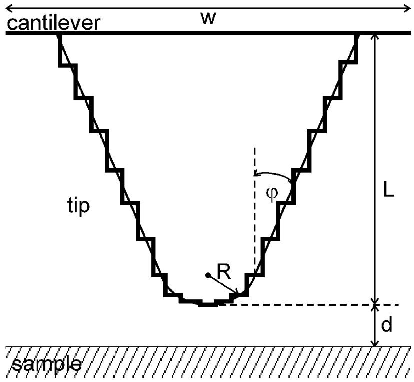

Fig. 1. Geometry for the simulation, defining the cantilever width *w*; the tip length, *L*; the tip radius, *R*; the cone half opening angle φ and the tip–sample distance *d*.

2.2. Simulation

The aim of the presented simulation is to obtain the dependence of the CPD resolution on the tip–sample distance (*d*) by means of a simple model (equivalent to a short computation time) and compare the results to the experiment. It is not intended to give an accurate description of the experimental situation. On this basis, a parallel plate model of the capacitive probe–sample system was adopted. The tip is described by a staircase, consisting of a parallel connection of simple parallel plate capacitors, following the shape of a truncated cone terminated by a sphere. Fig. 1 shows a schematic representation of the important geometric parameters. The dc voltage to be applied to compensate the CPD can be obtained by using [12]

$$\frac{\partial C}{\partial z} = \sum_i \frac{\partial C_i}{\partial z} \quad (2)$$

and setting Φ_ω from Eq. (1) to 0

$$V_{dc} = \frac{\sum_i (\partial C_i/\partial z)(\Delta\Phi_i/e)}{\sum_i (\partial C_i/\partial z)} \quad (3)$$

We modelled the pn-junction as a voltage step of size V_0,[1] and the steps on the surface as a potential line of

[1] Using the Schottky-model for the space charge region, the high doping concentration of the p- and n-type GaP results in a space charge region width of ~100 nm, which is neglected in the simulation.

height V_0. The step in the topography is neglected, since the step height is small compared to the tip–sample distance.[2] The system is treated as a metal–metal system, neglecting the effect of semiconductor surfaces, for which the voltage drop between tip and sample partly occurs in the semiconductor. In KPFM the effective applied voltage should be 0 due to the compensation of the CPD.

In the simulations the tip will be represented by a cone terminated by a sphere, using (see Fig. 1): cone half opening angle $\varphi = 20°$; tip length, $L = 15$ μm; cantilever width, $w = 24$ μm and tip radius, $R = 25$ nm. The cantilever is simulated as a square $w \times w$ neglecting the remaining part of the cantilever. Since the electrostatic force is measured by the oscillation of the cantilever at the second harmonic frequency, the outermost part of the cantilever will give the most important contribution.

3. Results

In Fig. 2 we show the cross-section of an UHV-cleaved GaP pn-junction exposing the (1 1 0) surface ($d \approx 6$ nm). In the topography (a) several steps and terraces can be seen on the left side (n-type) and a larger number of steps on the right side (p-type). This difference is presumably due to the liquid phase epitaxy growth of the p-type GaP layer. The work function image in Fig. 2(b) shows a clear contrast between the n-type ($\Phi_n \approx 4.6$ eV) and the p-type GaP ($\Phi_p \approx 5.7$ eV). The difference $\Delta\Phi \approx 1.1$ eV is smaller than expected (∼2.2 eV) from the high doping levels of the sample and was attributed to the effect of surface states on the (1 1 0) surface of GaP [15]. For the present study of the resolution this is not relevant, and we assume the difference in work function measured away from the junction as the total difference. In Fig. 2(c) an averaged linescan perpendicular to the junction is shown. The major part of the CPD change from the n- to p-type occurs within a few hundred nanometres, however, the CPD changes up to a distance of ∼2 μm, before showing a constant value.

[2] Due to the simultaneous measurement of CPD and topography, the tip maintains the same distance to the sample throughout the measurement.

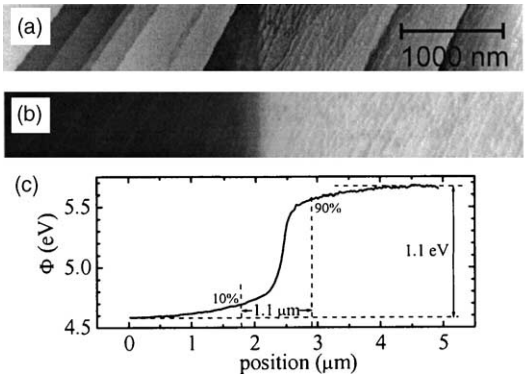

Fig. 2. KPFM results on the GaP pn-junction. (a) Topography (grey scale = 6.5 nm), (b) work function ($\Phi = 4.54 - 5.82$ eV) and (c) averaged line scan of the work function perpendicular to the junction.

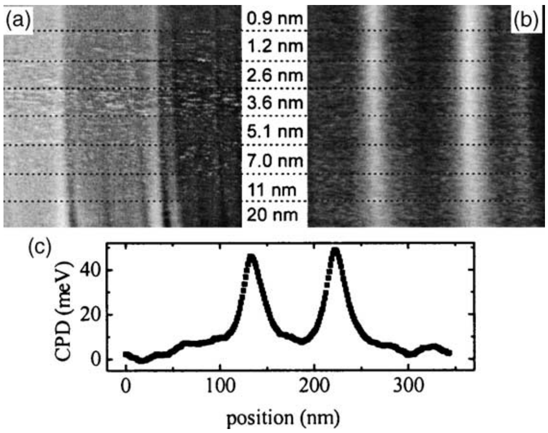

Fig. 3. KPFM measurements on GaAs(1 1 0). (a) Topography (grey scale = 0.8 nm) and (b) work function ($\Phi = 4.19 - 4.25$ eV). The same position was measured for different tip–sample distances, as indicated. (c) Averaged line scan through the CPD perpendicular to the steps ($d = 0.9$ nm).

Results of the experiments on the UHV-cleaved GaAs (1 1 0) surface are shown in Fig. 3. The topography shows a flat surface with two monolayer steps (step height ∼2.7 Å) along the (1 1 2) orientation. In Fig. 3(a) the topography is shown for different tip–sample distances, as indicated by the values in the figure. In Fig. 3(b), an increase of the work function along these steps is observed. The magnitude of the work function variation at the step increases with decreasing tip–sample distance. For clarity, we present in Fig. 3(c) an averaged linescan through the CPD perpendicular to the step direction, measured at a tip–sample distance of 0.9 nm. The work function increase at the step was attributed to surface states that induce band bending [13,15]; the (1 1 0) surface of GaAs is free of charged surface states and in flat band condition, however, at the steps this symmetry is interrupted.

Steps were also measured on the surface of highly oriented pyrolytic graphite (HOPG). On this metallic material a decrease in the work function along steps is found and interpreted by a dipole located at the step [13]. The determined distance-dependence of the size and the lateral width of the work function variation is presented and compared to the simulations in Fig. 5.

4. Discussion

The simulation of both samples, the pn-junction and the step induced work function variation, was performed for several tip sample distances. The results of the simulation of the potential step are presented in Fig. 4. We arbitrarily define the resolution of the simulated potential step as the distance between the points at which 10 and 90% of the full potential step is measured. The resolution decreases (10–90% value increases) with increasing tip–sample distance, showing values in the micrometer range for $d > 7$ nm. The inset in Fig. 4 shows that the resolution saturates at a value around 20 nm for small distances, indicating its

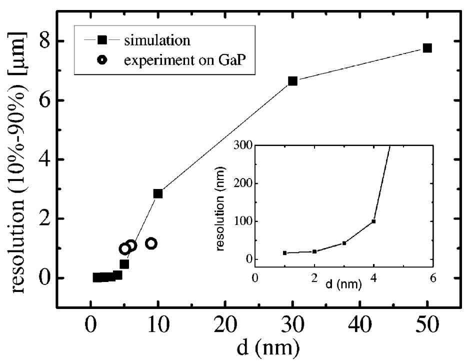

Fig. 4. Results from the simulation for the pn-junction modelled by a potential step of size V_0. The inset shows the resolution for small tip–sample distances. Open symbols represent the experimental data on the GaP pn-junction.

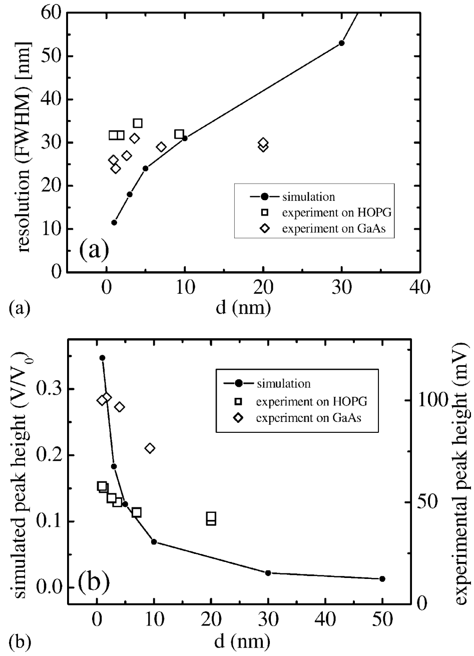

Fig. 5. Results from the simulation (closed circles) of the potential line (modelling the work function variation at steps): (a) lateral resolution and (b) peak height. The open symbols are the experimental results on GaAs and HOPG (right axis in (b)).

limitation by the tip radius. The experimental results (open circles in Fig. 4) are in agreement with the simulation, at least within the limited range of tip–sample distances studied.

In Fig. 5 we present the results of the simulations for the potential line, simulating the work function variation along the steps, where in (a) the lateral resolution (full width at half maximum (FWHM) of the CPD peak), and in (b) the dependence of the peak height on the tip–sample distance are shown. The simulation (filled circles) shows a decreasing resolution with increasing tip–sample distance; however, the resolution is still better than 100 nm for distances as large as 30 nm. As can be seen from Fig. 5(b), the magnitude of the measured work function change shows a much stronger dependence on the tip–sample distance. In fact, for distances above 30 nm the variation is nearly vanished (peak height $\sim 0.02V_0$), especially when considering the limited energy resolution (few meV) of a KPFM.

For KPFM in air, where large tip–sample distances are required due to the water film on the sample surface, these variations are very hard to resolve. The experimental results from our UHV-KPFM (open symbols) are in qualitative agreement with the simulation, as can be seen in Fig. 5(a) and (b). The lateral resolution is reproduced fairly well, whereas the increase of the peak height with smaller tip–sample distances shows deviations between experiment and simulation. The steeper increase for the simulation originates from the parallel plate capacitor model; the validity of this simplification is limited, especially at small tip–sample distances. From the similarity of the results on the metallic HOPG and the semiconducting GaAs, we conclude that the assumption of a negligible semiconductor effect is justified for this KPFM simulation.

5. Conclusion

We have presented measurements on the (1 1 0) surface of GaP and GaAs using KPFM in UHV. The potential drop across a pn-junction on GaP as well as the work function variation at steps on GaAs were imaged. The lateral and energy resolution as a function of tip–sample distance was compared to a simple staircase parallel plate capacitor simulation and found to be in reasonable agreement with the experimental results. Thus, this simple model helps to qualitatively evaluate experimental results. The resolution decreases considerably for tip–sample distances larger than about 10–30 nm. Thus, measurements with KPFM in air will suffer from considerable resolution deficiency, since larger tip–sample distances are required. Experiments where high resolution is required should preferably be performed in UHV.

Acknowledgements

The authors appreciate funding from the European Union under contract #HPRN-CT-2000-00031.

References

[1] R. Wiesendanger, Scanning Probe Microscopy and Spectroscopy: Methods and Applications, Cambridge University Press, Cambridge, 1994.
[2] J.M.R. Weaver, D.W. Abraham, J. Vac. Sci. Technol. B 9 (1991) 1559.
[3] M. Nonnenmacher, M.P. O'Boyle, H.K. Wickramasinghe, Appl. Phys. Lett. 58 (1991) 2921.
[4] A. Kikukawa, S. Hosaka, R. Imura, Appl. Phys. Lett. 66 (1995) 3510.
[5] S. Kitamura, K. Suzuki, M. Iwatsuki, Appl. Surf. Sci. 140 (1999) 265.
[6] S. Kitamura, K. Suzuki, M. Iwatsuki, C.B. Mooney, Appl. Surf. Sci. 157 (2000) 222.
[7] A.K. Henning, T. Hochwitz, J. Slinkman, J. Never, S. Hoffmann, P. Kaszuba, C. Daghlian, J. Appl. Phys. 77 (1995) 1888.
[8] A. Kikukawa, S. Hosaka, R. Imura, Rev. Sci. Instrum. 67 (1996) 1463.
[9] S. Belaidi, F. Lebon, P. Girard, G. Leveque, S. Pagano, Appl. Phys. A 66 (1998) S239.
[10] H.O. Jacobs, P. Leuchtmann, O.J. Homan, A. Stemmer, J. Appl. Phys. 84 (1998) 1168.
[11] G. Koley, M.G. Spencer, H.R. Bhangale, Appl. Phys. Lett. 79 (2001) 545.
[12] T. Hochwitz, A.K. Henning, C. Levey, C. Daghlian, J. Slinkman, J. Vac. Sci. Technol. B 14 (1996) 457.
[13] Ch. Sommerhalter, Th.W. Matthes, Th. Glatzel, A. Jäger-Waldau, M.Ch. Lux-Steiner, Appl. Phys. Lett. 75 (1999) 286.
[14] Ch. Sommerhalter, Th. Glatzel, Th.W. Matthes, A. Jäger-Waldau, M.Ch. Lux-Steiner, Appl. Surf. Sci. 157 (2000) 263.
[15] Th. Glatzel, S. Sadewasser, R. Shikler, Y. Rosenwaks, M.Ch. Lux-Steiner, Mater. Sci. Eng. B, in print (2003).